Eurasian J. Sci. Eng. Tech., 2025; 6(2): 072-081

Eurasian Journal of Science Engineering and Technology

Research article

www.dergipark.org.tr/tr/pub/ejset / www.dergipark.org.tr/en/pub/ejset

Investigation and production of the grooved part used in the crank pulley using finite element method

Cihangir Kaplan [1,*], Serkan Toros [2]

[1] *Kentpar Automotive, R&D Center, 42040, Konya, Türkiye*
[2] *Niğde Ömer Halisdemir University, Mechanical Engineering Department, 51240, Niğde, Türkiye*

Abstract

In recent years, crank pulleys have been manufactured using sheet materials in the automotive industry in line with cost and weight reduction targets. In this production process, sheet materials are first pre-formed and shaped and then a spinning process is applied to obtain the final form with a multi-grooved structure. In this study, 6224 (DD13) 3.5 mm thick sheet material, which is one of the hot rolled steels with low carbon content suitable for cold forming processes, was used. Using Simufact Sheet Metal Forming software, the isotropic Hill-48 material model and the anisotropic kinematic hardening model Chaboche were used to perform detailed analysis on the grooved part in the crank pulleys. The coefficients of the isotropic hardening model were determined from tensile test data and the parameters of Chaboche's kinematic hardening rule were determined from cyclic stress-strain test data. These curves, known as hysteresis cycles, were obtained from low repetition ±3%, ±7% and ±12% fatigue tests. For the determination of the Chaboche model parameters, a strain controlled and symmetrical experiment with one stable cycle was designed and produced. The data obtained from this scope were used as input to the analysis program. Analysis results and prototype manufacturing results were compared.

Keywords: Pulley, Spin forming, Finite element method, Sheet metal forming, Kinematic hardening, Chaboche

1 Introduction

Crank pulley is a torsional vibration damper used to reduce torsional vibration in internal combustion engines. In internal combustion engines, there are several types of vibration (axial, bending, etc.) on the crankshaft, but the most critical is torsional vibration. Since the crankshaft converts translational motion into rotational motion, torsional vibration causes life problems in combustion engines [1]. If this problem is not prevented, cracks and fractures in the crankshaft can be observed. In addition, high torsional amplitudes cause failures in other parts where the torque generated in the crankshaft is transmitted. In internal combustion engines, crank pulleys are used to prevent problems caused by torsional vibrations. With the advancement of technology, the ability of these pulleys to dampen vibrations has improved significantly, and today crank pulleys have been designed with different types of damping elements [2]. Despite these different types, the main purpose of the crank pulley is to reduce the torsional vibration level to an acceptable level [3]. Another purpose is to transfer torque from the engine through a belt to the water pump, air conditioning pump, and alternator. Crank pulleys are a component used in internal combustion engines to reduce torsional vibrations caused by irregular piston detonation while ensuring power transmission. These pulleys have tuned mass damping.

Nowadays, miniaturization of the engine, light weight of the engine and increasing the number of legs is becoming important demands in automobile production.

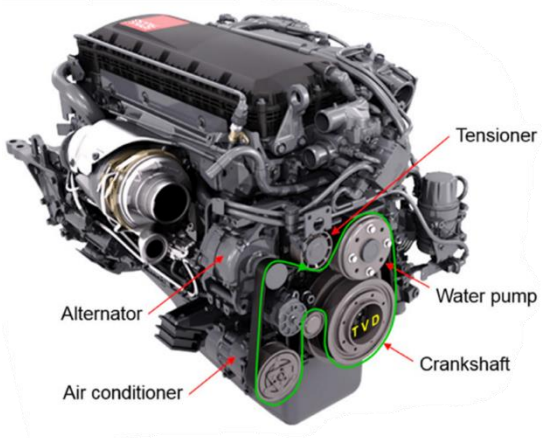

Figure 1. Engine front assembly representation [4]

Therefore, the grooved pulley has become an important component of the engine. It is widely used in automobiles, agricultural machinery, ships and other mechanical equipment. The traditional production methods of the grooved pulley leg are casting, tubular steel, solid steel and forging [5, 6]. The use of traditional production methods may result in the mechanical properties of the splined pulley part to be inferior. Conventional production methods produce low numbers of a splined part due to the high time per production run. The grooved pulley part produced by the spinning process replaces traditional production methods due to its advantages such as dimensional accuracy, pollution-free, high production efficiency, energy saving and

* Corresponding author, e-mail: kaplancihangir@gmail.com (C. Kaplan)
Received: 04.06.2025 Accepted: 24.07.2025 Published: 30.07.2025
doi: 10.55696/ejset.1714339

mechanical properties. The forming process of the grooved pulley part uses the spinning method found in sheet metal forming, in which rolled products are formed by pressing rollers onto the rotating workpiece [7]. The principal diagram of the grooved pulley part forming process is shown in Figure 2.

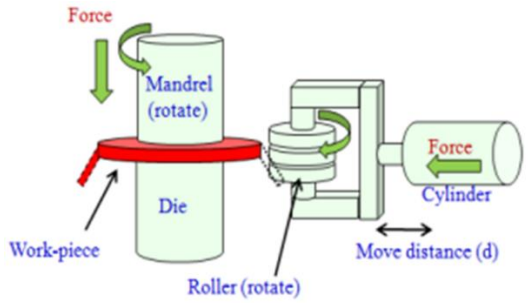

Figure 2. Sheet metal forming process with spinning method [5]

The workpiece is a circular sheet metal plate held between the die and the mandrel. The roller, which is a sheet metal working part, is connected to a rolling bearing and rotates around its own axis. The roller is moving towards the die part mandrel. The roller parts are pressed on the rotating workpiece and the sheet metal forming process is carried out. The forming process of the grooved pulley part consists of more than one pulley structure with different geometric shapes. The sheet metal forming procedure of the grooved pulley part consisting of four processes is shown in Figure 3.

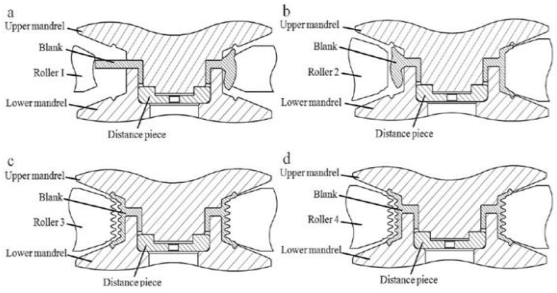

Figure 3. Grooved pulley manufacturing procedure consisting of four processes [6]

In the 1st operation, the spool, which resembles the geometric structure of the letter C, moves radially on the sheet metal and spinning is performed until the sheet metal takes the shape of a roller. The sheet metal moves up and down asymmetrically throughout the operation. This operation is known as sheet metal spinning. Figure 3. a show the operation visualization. In the 2nd operation, the roller, which looks like the geometric structure of the letter D, moves radially in the radial direction to fill the gap between the upper and lower mandrels to the sheet material, which is spinning in the amount determined in the first operation. This operation is known as flattening or flattening. The wall thickness of the sheet metal formed as a result of the operation is very important. Figure 3. b shows the operation visualization. In the 3rd operation, the roller with a rough groove shape structure moves in the radial direction and forms the first groove shape. This is known as the first groove forming operation. Figure 3. c shows the operation. In the 4th operation, the roller with the final groove shape structure moves in the radial direction to form the final groove shape. This operation process is called the final groove or final groove. Figure 3. d shows the operation. One period of the grooved pulley part forming process consists of several steps of sheet metal spinning, depending on the product types. During the pulley forming process, the workpiece deforms according to the shape of the pulley surfaces under the pressing of the pulleys. As a result of problems such as vibration, abrasion, inhomogeneity of the material, mandrel speed on the pulley, the product quality of the grooved pulley part deteriorates.

In the literature, many topics have been addressed for the grooved part in crank pulleys and kinematic stiffening analysis model. Xue et al. [8] analysed the material flow of the instantaneous part cross-section in the forming process of Poly-V grooved sheet metal material with Simufact Sheet Metal Forming program and the results were verified. Gądek et al. [9] convergence was made for the analysis and production results of the conical product forming on AA 1050A and DC04 steel with the Simufact program. The program provided 99.00% accuracy in production results. Pan et al. [10] used ABAQUS finite element analysis software to design a 3D model of a v-shaped pulley in their study. In the spinning process, the parameters affecting the quality of the hoop included working angle, corner radius, wall thickness reduction ratio, rotary feed rate, processing temperature. In this study, high accuracy was obtained by analyzing the effect of rotary working angle on spinning.

2 Material and methods

Empirical studies are carried out to determine the mechanical properties of materials. Tensile test is a method used to determine the mechanical properties of materials, especially under axial loads. As a result of the axially applied force a stress and strain curve results. Thanks to the stress and strain curve, properties that provide information about the mechanical behaviour of the material such as elongation, hardening, yield strength and tensile strength are determined. DD13 6224 sheet material, which is in high demand in sheet metal forming, is a hot rolling product and is continuously used in the automotive, defence industry and white goods sector. DD13 6224 sheet metal with a thickness of 3.5 mm was used in the study. The chemical components of DD13 6224 sheet material within the scope of the studies are given in Table 1. The material, whose basic alloying element is C, has significant advantages in terms of forming ability.

Table 1. Chemical properties of DD13 6224 sheet material

C (%)	Si (%)	Mn (%)	P (%)	S (%)	Cr (%)	Ni (%)	Cu (%)
0.038	0.017	0.268	0.018	0.007	0.023	0.024	0.026

2.1 Yield criteria

Tensile specimens were used for low carbon hot rolled steel DD13 6224 sheet material suitable for cold forming to be used in the metal spinning process. Tensile specimens were prepared in accordance with ASTM E8 standards. Tensile test pieces were produced according to the specimen design. They are shown in Figure 4. To perform tensile tests, specimens are placed between the jaws on the test machine. The specimen size values are checked and the data are entered into the software in the device. Based on the data entered, the test device is pulled in one direction and stress-strain values are obtained. Data is received with an excel file on the device. Although the load required for tensile is reduced, the true stress increases after yielding begins due to the further reduction of the area over which the load is applied. Engineering stress-strain data are used to obtain the true stress-strain graph. Figure 5 shows the actual stress-strain graph for DD13 6224 sheet material. In addition, the stress values are extrapolated until the plastic strain is 100% for use in simulations.

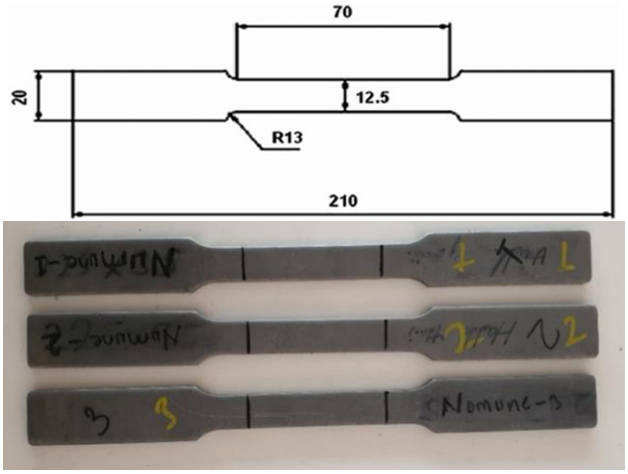

Figure 4. Design and product images of the tensile specimen [11]

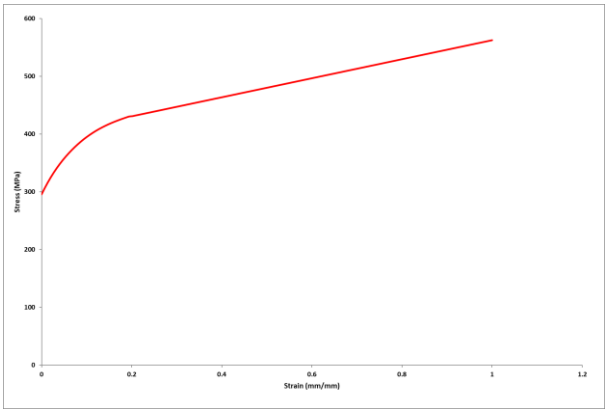

Figure 5. DD13 6224 true stress-strain graph

Another important model used in simulations of sheet metal forming processes is the yield surface models. Yield surface models are the models that determine that the material starts plastic deformation under multiaxial stresses that occur in multiaxial forming situations. Although there are many studies in this field in simulations, within the scope of this study, the analysis will be performed with reference to the anisotropic yield criterion in Simufact Forming software. This yield model is Hill-48 and the equation of the related model is given below [12].

$$f(\sigma_{ij}) \equiv F(\sigma_y - \sigma_z)^2 + G(\sigma_z - \sigma_x)^2 H(\sigma_x - \sigma_y)^2 + 2L\tau_{yz}^2 + 2M\tau_{zx}^2 + 2N\tau_{xy}^2 = 1 \quad (1)$$

Where f is the yield function, F, G, H, L, M, N are the anisotropy parameters of the material and x, y, z are the principal anisotropic axes. In the case where the principal axes of the stress tensor coincide with the anisotropic axes ($\sigma_x = \sigma_1$, $\sigma y = \sigma_2$, $\tau_{xy}=0$), the Hill-48 yield criterion depending on the principal stresses is given in Equation 2.

$$(\sigma_1^2) - \frac{2r_0}{1+r_0}\sigma_1\sigma_2 + \frac{r_0 + r_{90}}{r_{90}(1+r_0)}\sigma_2^2 = \frac{r_0(1+r_{90})}{r_{90}(1+r_0)} \quad (2)$$

The values obtained as a result of the calculations made according to the Hill-48 yield criterion are given in Table 2.

Table 2. Data obtained according to Hill-48 yield criteria

r0°	r45°	r90°	r_m	y0°	y45°	y90°
0.66	0.52	0.89	0.6475	296	312	300

2.2 Chaboche kinematic hardening model

The nonlinear kinematic stiffening models developed by Armstrong and Frederick allow a more accurate representation of plastic deformation behavior [13, 14]. In this framework, the Armstrong-Frederick model includes both stiffening and deformation in addition to Ziegler's classical equation. This model provides an important basis for nonlinear stiffening rules, especially expressed by the concept of back stress. In this context, Chaboche introduced a more advanced stiffening model by dynamizing the formula proposed by Armstrong and Frederick [15, 16]. Chaboche's model allows a more detailed modeling of complex loading-reloading behaviors by using multiple reverse stress components. They utilized isotropic-kinematic coupled stiffening models in finite element simulations for sheet metal forming process and showed that the new model they developed yielded results consistent with the experimental data obtained [17, 18].

There are many advantages to using both the original and modified Chaboche models to model the behaviour of the material under cyclic loading. The Chaboche model, including isotropic and kinematic stiffening, requires only four (for two back stresses) or six (for three back stresses) parameters associated with kinematic stiffening, two isotropic and some elastic parameters for most engineering applications. In addition, hardening parameters can be determined by uniaxial cyclic tensile/compression tests. Therefore, the number of experimental investigations can be

minimized. Tensile force at cyclically determined rates is applied to the test specimen. After the tensile force is applied, the process continues with compressive force. This tensile-compressive force is applied cyclically and repeatedly. Within the scope of this test study, a test specimen was designed. The thickness of the test sample is 3.5 mm. The technical drawing and cad data visualization of the test specimen are shown in Figure 6.

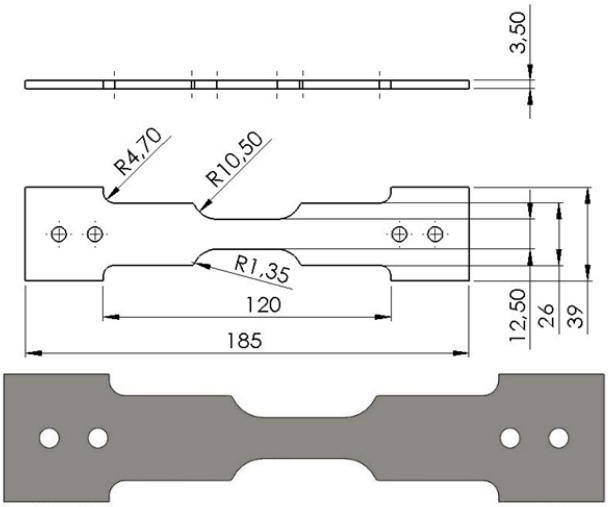

Figure 6. Cyclic loading sheet metal specimen technical drawing image and cad data image

In order to obtain accurate data during the cyclic loading test and due to the tendency of the test specimen to buckle during compression and tension, an apparatus was designed and manufactured for the test device. The apparatus to be connected to the cyclic loading sheet specimen consists of 2 parts. These are the upper table and the lower table. Apparatus design, cad data images and test specimen are shown in Figure 7.

A tensile-compression test bench is used for the determination of Chaboche parameters, but the experiment is carried out by repeated loading steps (cycling). Each tensile-compression operation is called a cycle. A cycle consists of loading steps such as initiation of tension, tensile loading and unloading, and then reverse loading and unloading. Chaboche parameters are obtained by nonlinear regression analysis. A single cycle is also sufficient for regression analysis. However, if the structure is actually subjected to how many repetitive loads, it is recommended to apply as many cycles during the experiment.

When modelling plastic deformation of metallic materials, the development of the yield surface can be taken into account by a translation and extension or expansion in the 3D stress space. For cold-formed parts, the accumulated plastic strain potentially influences the stress levels in subsequent cyclic loadings. In this sense, a combined isotropic-kinematic stiffening model can be put forward. In uniaxial form, the Von Mises yield function f is given for combined hardening [19].

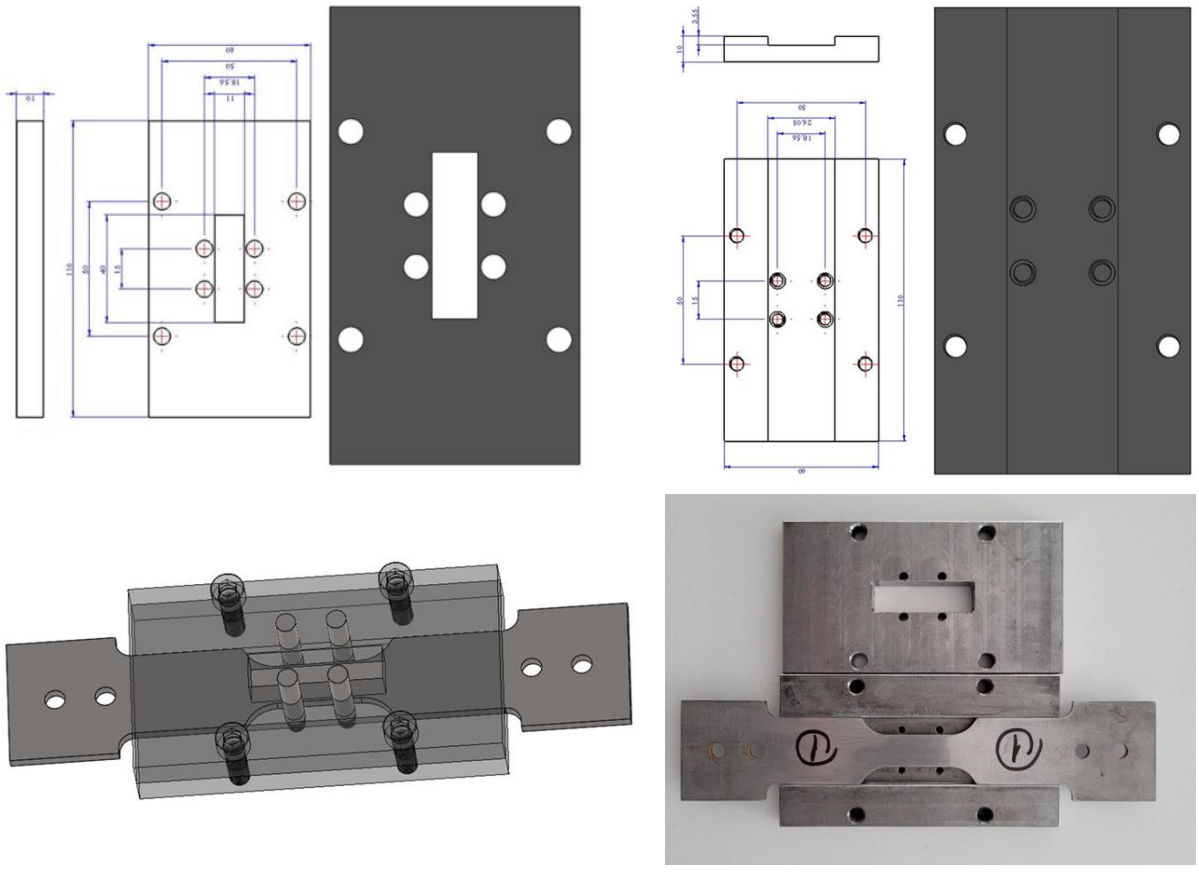

Figure 7. Apparatus upper and lower table technical drawing, cad data and product image

$$f=|\sigma-\chi|-k-R \quad (3)$$

Where f is the yield function, σ is the equivalent stress, χ is the back stress, k is the yield stress and R is the isotropic stiffening function. In this model, the nonlinear kinematic stiffening rule is determined according to the Armstrong and Frederick plasticity model [20]. It is given by the following expression:

$$\chi=\frac{C}{\gamma}\left(1-e^{-\gamma\varepsilon^{p}}\right) \quad (4)$$

Here ε^{p} is the plastic strain. γ and C are the kinematic stiffening material constants. In the Chaboche model, the kinematic stiffening rule is applied by considering multiple posterior stresses to extend the validity of this rule to a wider range of stresses and plastic strains [21].

Within the scope of cyclic load experimental studies, an apparatus design suitable for the test device was realized. A cavity was left as much as the thickness of the sheet metal in the test specimen apparatus. The specimen is mounted in the cavity. The specimen was designed and assembled in accordance with the upper and lower apparatus in the test machine. In this way, the test specimen was cyclically loaded to produce plastic deformation of 3%, 7% and 12%. The main purpose of this study is to determine the material's hardening characteristics under repetitive loading and to determine the parameters of the Chaboche material model, which is a kinematic hardening model.

Calculations were made based on the parameters mentioned above. Table 3 shows the results obtained. The data obtained from cyclic loading were calculated via Matlab and shown in the graph. Figure 8 shows the graph prepared via Matlab.

Table 3. DD13 Chaboche kinematic hardening model parameters

C (MPa)	γ
8923.5	101.899

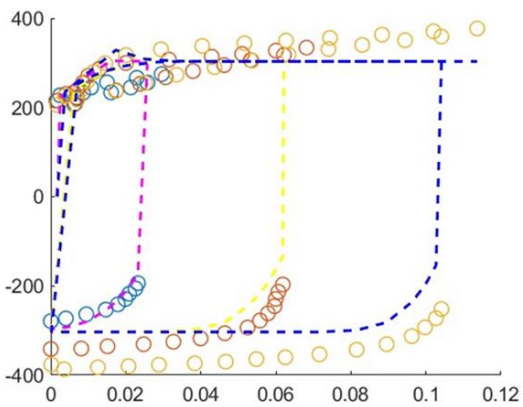

Figure 8. Graphical representation of the data determined for Chaboche

The Chaboche Hardening model, which has already been defined in Simufact Forming software, is defined in its simplest form. This model can be created in the form of a series with more C and γ values in order to reveal the non-linear hardening characteristics of materials, especially with the applied plastic deformation. However, since this is not available in the relevant software, calculations were performed with the assumption of linear kinematic hardening. Therefore, when the model prediction and experimental data are compared, the model prediction capability decreases with the progressive plastic deformation. In this case, it means that the material has linear hardening characteristics.

3 Results and discusion

Simulation method of plastic forming deformation process has also made remarkable progress with the development of experiment and theoretical analysis, and has significantly helped scientific research and actual production. Finite element simulation is easily used to simulate a process in real production, prototyping, observing the occurrence of relevant factors and evaluating the operation process. Examining the results of the analysis by conducting multiple analysis studies allows it to give an idea before production. In this way, problems to be experienced in production are minimized.

The spinning process analysis studies were carried out using the Sheet Metal Forming Module of the Simufact program. Die elements in the system are considered rigid. The surface interactions between the die elements and the sheet material were modelled according to Coulomb's Rule. According to this law, the friction coefficient was taken as 0.1 in the analysis. In the finite element analysis model, the temperatures of the sheet/workpiece and die parts were taken as 20 °C. Adiabatic heating due to plastic deformation and temperature increases due to friction and its effects on the mechanical behaviour of the sheet material are ignored. Figure 9 shows a visual representation of the analysis program.

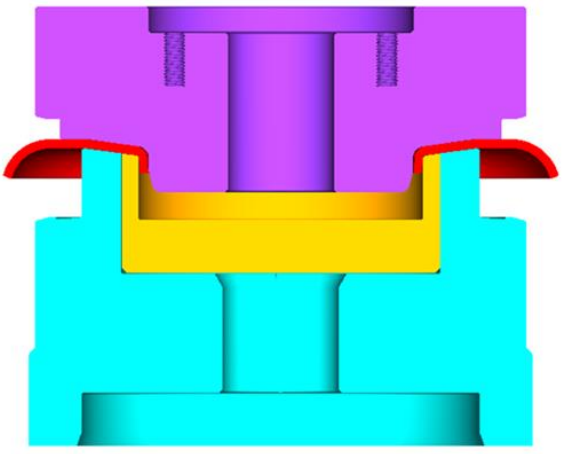

Figure 9. Simufact sheet metal forming analysis die image

Finite Element method is used for workpiece modelling in which the analysis model is divided into basic elements consisting of small parts. This process is called mesh structure. Each element has a node structure at the corners. Calculations are performed by working on these nodes and analyses are performed. A mesh structure was created for the workpiece to be used in the analysis studies. The mesh type of the workpiece is Advancing Front Quad and the element type is Quads (10). Element size was chosen as 0.15. In this way, the workpiece has 10549 elements. Figure 10 shows the mesh structure visualization of the workpiece.

Figure 10. Mesh structure visualization of the workpiece

Technical drawings are needed for the production of the grooved part of the crank pulley. Within the scope of the study, the drawings of the grooved part to be produced within the scope of the study were made in the Solidworks program and a technical drawing with geometric dimensions was prepared. Figure 11 shows the technical drawing of the grooved part.

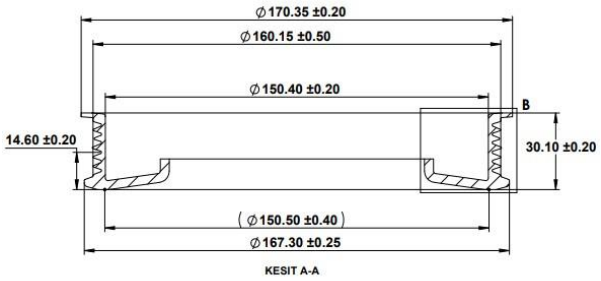

Figure 11. Technical drawing visualization of the grooved part

Descriptions were made for the visuals of the analysis and production results. In the pictures, a indicates Isotropic Analysis Result, b indicates Kinematic Hardening Result and c refers to Production Result. The technical drawing to be used in the production of the grooved part is examined and the length dimension value is given. The Length dimension of the product is 30.10 ± 0.20 mm. When two different analysis and production results are examined, the value of 29.95 mm was obtained as a result of isotropic analysis, 30.00 mm value was obtained in the analysis made with kinematic hardening data, while the value of 30.04 mm was found as a result of the measurement of the groove part produced on the CNC spinning machine with a gauge. The analysis and production result visuals of the product are given in Figure 12. Table 4 includes detail data.

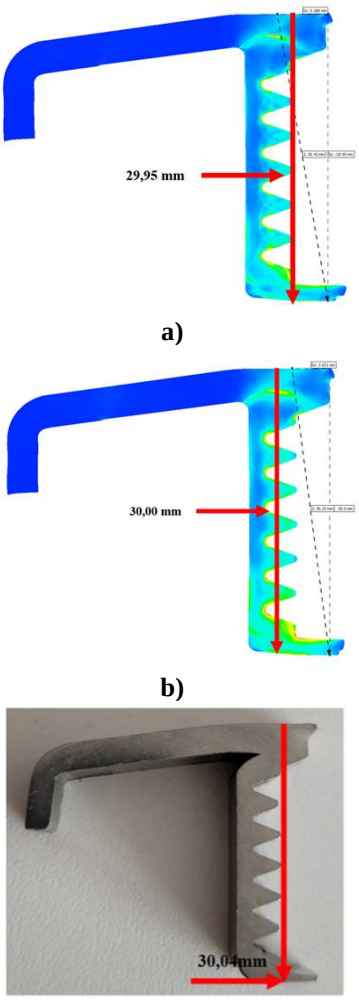

Figure 12. Length analysis and production measurement reports of the grooved part

Table 4. Length dimension

	Length Dimension			
	Minimum Dimension (mm)	**Nominal Dimension (mm)**	**Maximum Dimension (mm)**	**Results**
Isotropic Analysis Result	29.90	30.10	30.30	29.95
Kinematic Hardening Result	29.90	30.10	30.30	30.00
Production Result	29.90	30.10	30.30	30.04

Figure 11, which shows the geometric dimensions of the ducted part, is examined, the top diameter of the duct should be Ø160.15 ± 0.50 mm. The results of two different analysis studies and production were examined. As a result of the isotropic analysis, the diameter of the top of the groove was Ø160.34 mm, and Ø160.44 mm was obtained as a result of the analysis studies with kinematic hardening data. After the production of the grooved part, its dimensional measurements were taken on the CMM machine. As a result

of the measurement, Ø160.48 mm over groove diameter value was found. The analysis and production result visuals of the product are given in Figure 13. Table 5 includes detail data.

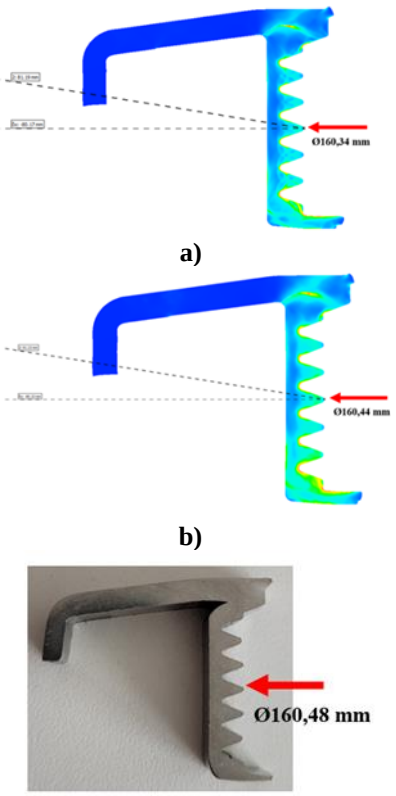

Figure 13. Analysis and production measurement reports of the groove top diameter of the grooved part

Table 5. Groove top diameter dimension

	Groove Top Diameter Dimension			
	Minimum Dimension (mm)	**Nominal Dimension (mm)**	**Maximum Dimension (mm)**	**Results**
Isotropic Analysis Result	159.15	160.15	160.65	160.34
Kinematic Hardening Result	159.15	160.15	160.65	160.44
Production Result	159.15	160.15	160.65	160.48

In the technical drawing of the grooved part, the inner diameter value is given as Ø150.40 ± 0.20 mm. While the inner diameter obtained as a result of isotropic analysis was Ø150.26 mm, the value of Ø150.36 mm was found as a result of analysis with kinematic hardening data. After the manufacture of the grooved part, geometric dimensions were taken on the CMM measuring machine and a value of Ø150.40 mm was obtained. A comparison was made between the data of the analysis studies and the technical drawing dimensions. The analysis and production result visuals of the product are given in Figure 14. Table 6 includes detail data.

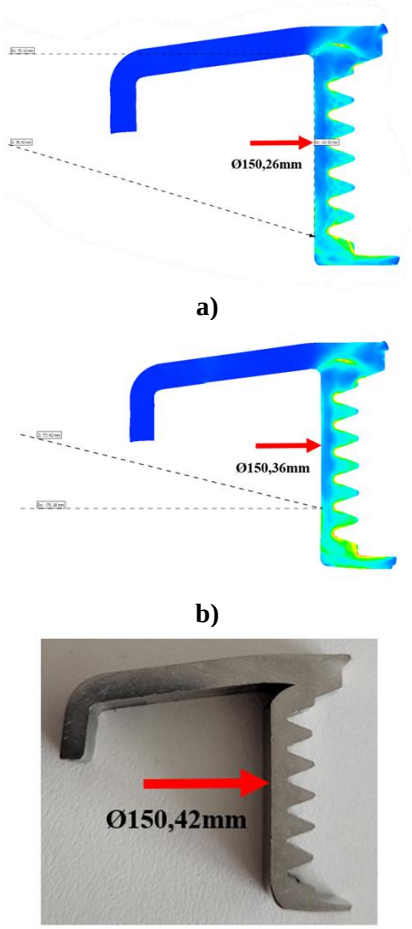

Figure 14. Analysis and production measurement reports of the inner diameter of the grooved part

Table 6. Inner diameter dimension

	Inner Diameter			
	Minimum Dimension (mm)	**Nominal Dimension (mm)**	**Maximum Dimension (mm)**	**Results**
Isotropic Analysis Result	150.20	150.40	150.60	150.26
Kinematic Hardening Result	150.20	150.40	150.60	150.36
Production Result	150.20	150.40	150.60	150.42

Groove distance value has an important dimension in crank pulleys. The groove distance must be produced within the given geometric tolerance dimensions. If the product is produced outside the groove distance dimension, it affects the life of the belt-pulley system in internal combustion engines. Materials such as alternator pulley, air conditioner

pulley, etc. on the system cause effects on the belt. Within the scope of analysis studies, this measurement is determined according to the assembly of the pulleys. The analysis and production result visuals of the product are given in Figure 15. Table 7 includes detail data.

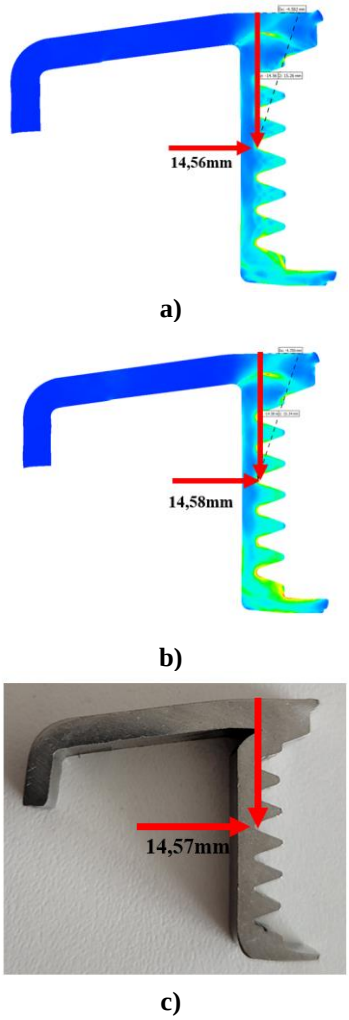

Figure 15. Analysis and production measurement reports of groove distance

Table 7. Groove distance dimension

	Groove Distance			
	Minimum Dimension (mm)	**Nominal Dimension (mm)**	**Maximum Dimension (mm)**	**Results**
Isotropic Analysis Result	14.40	14.60	14.80	14.56
Kinematic Hardening Result	14.40	14.60	14.80	14.58
Production Result	14.40	14.60	14.80	14.57

Roller designs were made by considering the technical drawing values given for production. The upper diameter is determined by the movement of rollers 2, 3 and 4 in radial direction. In the analysis studies, an estimate was made for Ø167.30 ±0.25 mm. While Ø167,16 mm value was obtained as a result of isotropic analysis, Ø167,26 mm value was found in the anisotropic kinematic consolidation model. Ø167,30 mm value was obtained after the production studies on CNC spinning machine. The analysis and production result visuals of the product are given in Figure 16. Table 8 includes detail data.

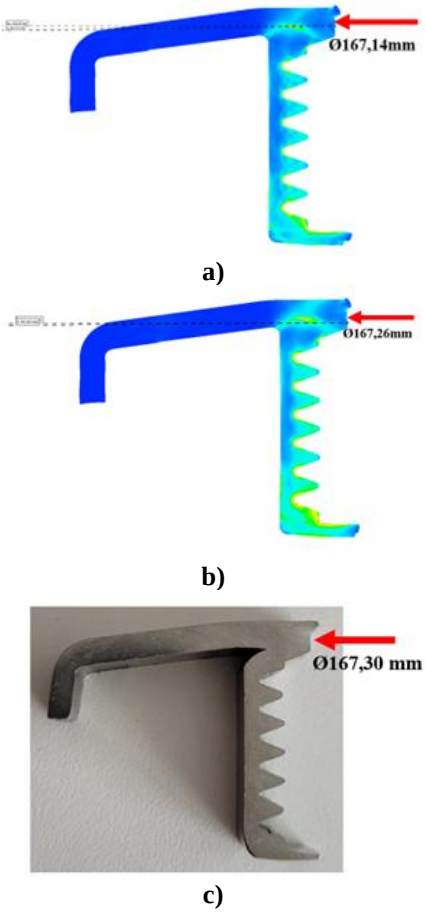

Figure 16. Analysis and production measurement reports of the upper diameter of the grooved part

Table 8. Upper diameter dimension

	Upper Diameter			
	Minimum Dimension (mm)	**Nominal Dimension (mm)**	**Maximum Dimension (mm)**	**Results**
Isotropic Analysis Result	167.05	167.30	167.55	167.14
Kinematic Hardening Result	167.05	167.30	167.55	167.26
Production Result	167.05	167.30	167.55	167.30

In the grooved part, the bottom diameter varies according to the sheet metal flow. Different values are obtained according to the radial advance and position of the rollers. If

there is not enough diameter in the grooved part, it causes the grooved not to be formed in standard dimensions. In the technical drawing, this dimension is given as Ø170.35 ± 0.20 mm. While Ø171.38 mm was obtained in isotropic analysis studies, Ø170.32 mm was found in the anisotropic kinematic hardening model. The analysis and production result visuals of the product are given in Figure 17. Table 9 includes detail data.

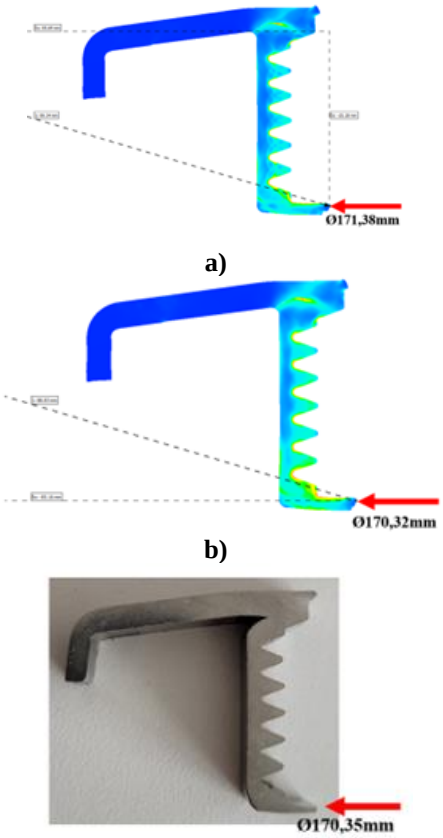

Figure 17. Analysis and production measurement reports of the bottom diameter of the grooved part

Table 9. Bottom diameter dimension

	Bottom Diameter			
	Minimum Dimension (mm)	**Nominal Dimension (mm)**	**Maximum Dimension (mm)**	**Results**
Isotropic Analysis Result	170.15	170.35	170.55	171.38
Kinematic Hardening Result	170.15	170.35	170.55	170.32
Production Result	170.15	170.35	170.55	170.35

4 Conclusions

As a result of the studies, analysis studies were carried out with both isotropic and kinematic stiffening model of the grooved part used in a crank pulley. In the light of the analysis studies, the necessary comparisons were obtained by producing the die designed in the light of the analysis studies and at the same time producing the final product on the spinning machine. When the final product production and the results of two different analyses were compared, the Chaboche kinematic hardening model showed a better prediction performance in the analysis.

Conflict of interest

The authors declare that there is no conflict of interest.

Similarity rate (iThenticate): 14%

References

[1] Londhe, Abhijit, and Vivek H. Yadav, ‘‘Design and optimization of crankshaft torsional vibration damper for a 4-cylinder 4-stroke engine,’’ No. 2008-01-1213, SAE Technical Paper, 2008. https://doi.org/10.4271/2008-01-1213.

[2] W. Homik, ‘‘Damping of torsional vibrations of ship engine crankshafts-general selection methods of viscous vibration damper’’, Polish Maritime Research 18(3), 43-47, 2011. https://doi.org/10.2478/v10012-011-0016-9.

[3] G. Nerubenko, ‘‘Torsional Vibration Damper with Micro-channel Tuners’’, No. 2014-01-1691, SAE Technical Paper, 2014. https://doi.org/10.4271/2014-01-1691.

[4] C. Silva, L Manin, R Rinaldi, E. Besnier and D. Remond, ‘‘Dynamics of Torsional Vibration Damper (TVD) pulley, implementation of a rubber elastomeric behavior, simulations and experiments’’, Mechanism and Machine Theory 142, 103583, 2019. https://doi.org/10.1016/j.mechmachtheory.2019.103583.

[5] H. S. Park, V. V. Hoang, J. Y. Song, D. H. Kim and N. T. Le, ‘‘A Concept of SelfOptimizing Forming System’’, Journal of the Korean Society of Manufacturing Technology Engineers 22(2), 292-297, 2013.

[6] K. Xue, J. Zhou, S. Yan and P. Li, ‘‘Flow diversion mechanisms and control methodology in asymmetric spinning of special-shaped multi-wedge belt pulley’’, The International Journal of Advanced Manufacturing Technology,1-14,2022. https://doi.org/10.1007/s00170-020-05496-3.

[7] Q. Zhang, C. Zhang, M. J. Zhang, C. C. Zhu, S. Q Fan and S. D. Zhao, ‘‘Research of net-shape power spinning technology for poly-V grooved aluminum pulley,’’ The International Journal of Advanced Manufacturing Technology 81, 1601-1618, 2015.

[8] Xue, K., Wu, C., Yang, W., Dai, G., Li, P., & Yan, S. ‘‘Study on Rotary Bending Forming Process of Torsional Damper Shell Pulley’’, Xibei Gongye Daxue Xuebao/Journal of Northwestern Polytechnical University, 37(5), 1053-1059, 2019. https://doi.org/10.1051/jnwpu/20193751053.

[9] Gądek, T., Majewski, M., & Sułek, B., ‘‘Reverse Engineering Of The Metal Spinning Process For Conical Angle 163° Using Fem With Simufact

Formıng'', International Journal of Modern Manufacturing Technologies (IJMMT), 16(2), 2024.
[10] Pan, Y., Xueguang, L., Zhe, C., & Yang, Y., ''Roller spinning forming regularity'', Journal of Measurements in Engineering, 5(4), 229-234, 2017.
[11] ASTM, E8–99, ''Standard test methods for tension testing of metallic materials'', Annual book of ASTM standards, ASTM (2001).
[12] Lian, J., Shen, F., Jia, X., Ahn, D. C., Chae, D. C., Münstermann, S., & Bleck, W., ''An evolving non-associated Hill48 plasticity model accounting for anisotropic hardening and r-value evolution and its application to forming limit prediction'', International Journal of Solids and Structures, 151, 20-44, 2018. https://doi.org/10.1016/j.ijsolstr.2017.04.007.
[13] Armstrong P.J. ve Frederick C.O., ''A mathematical representation of the multiaxial Bauschinger effect'', Mater. High Temp., 24 (1), 1-26, 2007. https://doi.org/10.3184/096034007X207589.
[14] Chaboche J.L., ''Constitutive-equations for cyclic plasticity and cyclic viscoplasticity'', Int. J. Plast., 5 (3), 247-302, 1989. https://doi.org/10.1016/0749-6419(89)90015-6.
[15] Bouhamed A., Jrad H., Said L.B., Wali M., Dammak F., ''A non-associated anisotropic plasticity model with mixed isotropic-kinematic hardening for finite element simulation of incremental sheet metal forming process'', Int. J. Adv. Manuf. Technol., 100 (1), 929-940, 2019. https://doi.org/10.1007/s00170-018-2782-3.
[16] Moslemi N., Gol Zardian M., Ayob A., Redzuan N., Rhee S., ''Evaluation of sensitivity and calibration of the Chaboche kinematic hardening model parameters for numerical ratcheting simulation'', J Appl Sci, 9, 2578, 2019. https://doi.org/10.3390/app9122578.
[17] Mahmoudi A.H., Badnava H., Pezeshki-Najafabadi S.M., ''An application of Chaboche model to predict uniaxial and multiaxial ratcheting'', Procedia Eng., 10, 1924-1929, 2011. https://doi.org/10.1016/j.proeng.2011.04.319.
[18] Badnava H., Pezeshki S.M., Fallah Nejad K., Farhoudi H.R., ''Determination of combined hardening material parameters under strain controlled cyclic loading by using the genetic algorithm method'', J. Mech. Sci. Technol., 26 (10), 3067-3072, 2012. https://doi.org/10.1007/s12206-012-0837-1.
[19] Chaboche, J. L., ''Modelization of the strain memory effect on the cyclic hardening of 316 stainless steel'', In Transactions of the 5th International Conference of SMIRT, Berlin, 1979.
[20] Araujo, M. C., ''Non-linear kinematic hardening model for multiaxial cyclic plasticity'', Louisiana State University and Agricultural & Mechanical College, http://doi.org/10.31390/gradschool_theses.1650.
[21] Halama, R., Sedlák, J., & Šofer, M., ''Phenomenological modelling of cyclic plasticity'', Numerical modelling, 1, 329-354, 2012. http://doi.org/10.5772/35902.